Cite as:
Holder, S.J., Jones, R.G. in *Silicon Based Polymers: Advances in Synthesis and Supramolecular Organization*, Eds. Ganachaud, F., Boileau, S., Boury, B., **2008**, 249-277. DOI: 10.1007/978-1-4020-8528-4_18

The Synthesis, Self-Assembly and Self-Organisation of Polysilane Block Copolymers

S. J. Holder and R. G. Jones

Functional Materials Group, School of Physical Sciences, University of Kent, Canterbury, Kent. CT2 7NH. UK.

1. Introduction

Polysilanes are linear polymers with a backbone of catenated silicon atoms that are usually substituted with aryl and/or alkyl groups [1]. Polysilanes display electronic delocalization within the σ-bonded framework of the Si-Si backbone as a consequence of sp^3 orbital interactions between Si atoms (the smaller dimensions of the hybrid orbitals of the carbon atoms preclude this delocalization in analogous unsaturated C-C polymer backbones). This electron delocalization plays a large part in determining the properties of polysilanes, in particular the spectroscopic, and electroactive properties. As a consequence they have potential applications as semiconducting [2], photoconducting [3, 4], electroluminescent [5, 6], and non-linear optical materials [7]. They have found applications as precursors to β-SiC fibres [8, 9], as resists in microlithography [10, 11], and as photoinitiators of radical polymerization [12]. However, their mechanical properties are relatively poor, adversely affecting their processability and limiting their exploitation. In order to exploit their properties, attempts have been made to combine polysilanes with organic polymers with complementary characteristics in order to optimise mechanical properties. Whilst many structural properties can be optimised through the incorporation of two or more polymer components in a copolymer structure, block copolymers are also being increasingly studied as self-organising and self-assembling materials. The microphase separation of block copolymers gives a wide range of 3-dimensional morphologies in the bulk state [13] and the self-

assembly of block copolymers in different liquid media give a variety of aggregate structures such as vesicles [14], micelles [15], and micellar fibres [16]. A number of applications have been demonstrated for block copolymer aggregate structures including their use as encapsulants for drug delivery [17] and templates for colloid synthesis [18]. It has been demonstrated, that the self-assembly and/or self-organisation of block copolymers might be used for the imposition of increased order to fine-tune the performance of conjugated polymers and facilitate the preparation of nano-scale devices [19]. Polysilanes as σ-conjugated polymers are therefore ideal targets for investigation as self-organizing and assembling block copolymer systems. Polysilanes are rod-like, they have semi-rigid, segmented backbones that ensue from their σ -conjugated chains and helical conformations [20, 21]. Thus, they offer a significant potential for self-alignment that tends to be similar to that for π-conjugated carbon based block copolymers. They also offer the possibility of bringing to block copolymer structures the characteristic properties that result from their σ-conjugation and, hence, access to new structure-property combinations through self-organization in bulk or self-assembly through aggregation. This paper will review the methodologies that have been developed for the synthesis of polysilane block copolymers, the resultant morphologies in thin films and their self-assembly in solution, and highlight some of their more interesting properties and applications.

2. Synthesis

2.1. Synthesis of Polysilane Blocks

Most but not all strategies for the synthesis of block copolymers based on polysilanes require pre-syntheses of the polysilanes that will comprise the blocks. Thereafter, the other copolymer component blocks are attached to the polysilane (a

polymer coupling approach) or else grown from its appropriately functionalized chain ends (a living polymerization approach). There are four known procedures for the synthesis of polysilanes (Figure 1), the Wurtz-type reductive-coupling of dichloroorganosilanes [22] (Reaction 1), the ring-opening of cyclosilanes [23] (Reaction 2), the anionic polymerization of 'masked' disilenes [24] (Reaction 3) and the catalytic dehydrogenation of primary silanes [25] (Reaction 4). For detailed descriptions of these procedures the reader is referred to recent reviews [26]. Of these approaches the catalytic dehydrogenation has yet found no application in the synthesis of block copolymers. This is principally because high molecular weight polysilanes are only obtained from the dehydrocoupling of tertiary organosilanes and the resultant polymers possess no discrete end-group functionalities for subsequent polymer coupling or polymerization initiation.

Both the anionic polymerization of masked disilenes and the ring-opening polymerization are living polymerizations under the appropriate conditions and hence after full monomer conversion they retain silyl anion end-functions suitable for block copolymer synthesis. Both of these polymerizations can give quantitative yields of polysilane with narrow molecular weight distributions and molecular weight parameters controlled by the ratio of monomer to initiator. However in both cases the monomers require careful and time-consuming multi-step syntheses. In contrast the Wurtz-reductive coupling polymerization under the appropriate conditions, can give polysilanes in high yields utilizing commercially available monomers and reagents [27]. Furthermore the end-groups are predominantly Si-Cl bonds which are ideal for subsequent use in block copolymer syntheses. The principal disadvantage of the Wurtz-reductive coupling polymerization is that whilst it can be controlled to give monomodal samples, it gives polysilanes with high polydispersities (typically 1.5-2 under optimum conditions) with yields no higher than 50-80% under optimum conditions.

2.2. Synthesis of Polysilane Block Copolymers

2.2.1 Polymer Coupling Reactions

The use of polysilanes as photoinitiators of radical polymerization was one of the first means whereby they were incorporated within block copolymer structures [28], albeit in an uncontrolled fashion. However the resulting block copolymer structures were poorly defined and interest in them principally lay in their application as compatibilisers for polystyrene (PS) and polymethylphenylsilane blends PMPS. The earliest synthetic strategies for relatively well-defined copolymers based on polysilanes exploited the condensation of the chain ends of polysilanes prepared by Wurtz-type syntheses with those of a second prepolymer that was to constitute the other component block. Typically, a mixture of AB and ABA block copolymers in which the A block was polystyrene (PS) and the B block was polymethylphenylsilane (PMPS) was prepared by reaction of anionically active chains ends of polystyrene (e.g. polystyryl lithium) with Si-X (X = Br, Cl) chain ends of α,ω-dihalo-polymethylphenylsilane [28] an example of which is shown in Figure 2 [29, 30]. Similar strategies were subsequently used to prepare an AB/ABA copolymer mixture in which the A block was poly(methyl methacrylate) (PMMA) [31] and also a multi- block copolymer of PMPS and polyisoprene (PI) [32].

A particularly interesting block copolymer made by the coupling approach was a multi-block copolymer of PMPS and poly(ethylene oxide) (PEO). This was prepared by reacting the Si—X chain ends of PMPS with the hydroxyl chain ends of well-defined commercial sample of poly(ethylene glycol) [32] (Figure 3). Although the former had a normal molecular weight distribution, the latter was of a uniform distribution. As determined by size exclusion chromatography, the resul-

tant copolymer consisted of all the $(AB)_n$ and $(AB)_nA$ structures from PMPS-PEO through to $(PMPS\text{-}PEO)_{16}$.

2.2.2 Living Polymerizations

The polymer coupling approach to block copolymer synthesis is seriously disadvantaged by the need to ensure stoichiometric equivalence of the reactive functional groups. These are in low concentration relative to the main chain units of the polymer chains and they are usually sensitive to trace impurities, particularly water (e.g. Si-Cl rapidly converts to Si-OH, Si^- rapidly converts to Si-H) Hence obtaining stoichiometric equivalents of the chain ends is extremely difficult and leads to poor reproducibility without scrupulous care using high vacuum line procedures. In contrast, the living polymerization approach either (i) uses the reactive chain end of a preformed polysilane to initiate polymerization of a vinyl monomer; (ii) uses the reactive chain end of a preformed polysilane to functionalize the chain with a suitable initiator for a subsequent living polymerization; (iii) a polymeric carbanion (e.g. polystyryl lithium) is used to initiate the polymerization of the silane monomer. The resulting block copolymer structures are usually more defined than those prepared by polymer coupling and copolymers based on polysilanes with both AB and ABA structures have been synthesized these ways.
The first such living polymerization syntheses were achieved using the living silyl-anionic chain ends on poly(1,1-dihexyl-2,2-dimethylsilane) and poly(1-butyl-1,2,2- trimethylsilane), prepared using the masked disilene procedure [24], to initiate the polymerization of methyl methacrylate, trimethylsilyl methacrylate and 2-(trimethylsilyloxy) ethyl methacrylate [33-35] (Figure 4a). A further example of the synthetic utility of this approach came with the synthesis of poly(1,1-dimethyl-2,2-dihexyldisilene)-*b*-poly(triphenylmethyl methacrylate) (PMHS-*b*-PTrMA) [60]. The PTrMA block was synthesized in the presence of (-)-sparteine which induced the adoption of a helical conformation in the methacrylate block, i.e. a chiral one-handed helical chain. When the temperature was reduced to -20ºC the poly-

silane chain was induced by this block to adopt a one-handed helix itself and become chiral and optically active itself.

PMPS-*b*-PS and PMPS-*b*-PI were synthesized by the anionic ring-opening polymerization of tetramethyltetraphenylcyclotetrasilane (prepared from commercially available octaphenyltetrasilane) initiated by the living anionic chain ends of polystyrene and polyisoprene [36] (Figure 4b).

Over the past 10 years the advent of controlled radical polymerization has resulted in an explosion of interest in the synthesis of block copolymer systems that were hitherto inaccessible [37]. The most commonly used methods of controlled radical polymerization of vinyl monomers are nitroxyl mediated (e.g. TEMPO), reversible addition fragmentation (RAFT) and atom transfer radical polymerization (ATRP) [38]. Both TEMPO and ATRP based syntheses of polysilane block copolymers have been reported. Poly(styrene-*block*-methylphenylsilane-*block*-styrene) has been synthesized by a TEMPO-mediated polymerization from an end functionalized PMPS macromolecular initiator (Figure 5) [39]. The first inorganic–organic hybrid copolymer system synthesized via ATRP was that of polystyrene grafts grown from a bromomethylated PMPS sample [40]. A more generally useful approach has been the end-functionalization of PMPS with an active ester alkyl halide 2-bromo-2-methyl propanoate followed by its application in the copper catalyzed ATRP of methyl methacrylate, hydroxyethyl methacrylate and oligo(ethylene glycol methyl ether methacrylate) (Figure 6) [41, 42]., In these cases the precursor α,ω-dihaloPMPS was of a broad polydispersity (typically 1.6-2.1) which was reacted with hydroxyethyl 2-bromo-2-methylpropanoate to give end-functionalized PMPS (characterized by ^{1}H NMR). A variety of PMPS molecular weights were prepared in this manner and the appropriate vinyl monomers were polymerized using a Cu(I)Br catalyst and a bidentate N-containing ligand (e.g pyridine) in a solvent (e.g. THF). The resultant ABA block copolymers were of lower polydispersities than the precursor PMPS blocks as expected from the incorporation of narrow distribution blocks at the chain ends of a sample with a formerly broad distribution. The molecular weight parameters measured by SEC were in

broad agreement with the theoretical M_n values predicted from consideration of the monomer to initiator ratios and were observed to grow in a manner consistent with a controlled chain growth polymerization (Figure 7a). Kinetic analyses ($\ln[M_0]/[M]$ versus time) of the polymerization of MMA from a PMPS macroinitiator clearly demonstrated 1st order behaviour as expected from ATRP (Figure 7b).

3. Self-Assembly and Self-Organization of Polysilane Block Copolymers

3.1 Self-Organization in Thin Films

The ability of copolymers consisting of chemically distinct polymeric segments to undergo microphase separation as a result of enthalpically driven segregation has led to a remarkable range of nanostructured morphologies being catalogued and studied [43]. Consequently, such materials have been the subject of intense study for over ten years [44]. Block copolymer thin films show many of the morphologies displayed by the bulk materials, but substrate and surface effects can play a much more pronounced role in the self-organization, particularly for very thin films. A large number of potential applications for these self-organizing thin films have been proposed and demonstrated. Examples include applications as lithographic masks [45], photonic materials [46], and nanostructured membranes [47].

Demoustier-Champagne et al. used atomic force microscopy (AFM) to observe microphase separation within cast films of PS-PMPS-PS/ PS-PMPS block copolymer mixture [29] that were used to compatibilize a blend of PMPS and PS. The fracture surface of blend films with the block copolymer incorporated show a far

finer dispersion of particle sizes than those without. Matyjaszewski et al. studied PMPS-PS thin films by SFM (scanning force microscopy) and TEM (transmission electron microscopy) and Figure 8 shows a TEM picture of a thin section of a film which was prepared by slow evaporation from THF, which is slightly selective for the polystyrene block [48]. The dark areas were assigned to the polysilane domains as a result of the stronger electron scattering in silicon rich regions compared to carbon rich regions. The domains were poorly defined but multiple images demonstrated that the morphology was real. The wormlike dark domains were consistent with a cylindrical morphology of the polysilane block in a matrix of polystyrene. The cylinders had approximately the same size throughout the entire sample with a diameter of 7±2 nm. This was roughly half of the extended chain length of 14.8 nm of the PMPS component (M_n = 9,000) of the block copolymer. Intriguingly by exposing a thin film of the PMPS-PS block copolymer to UV light of 360nm the PMPS could be selectively degraded. Whilst initial SFM analysis of the film revealed no change in texture over the surface after UV exposure bundles of the PI became apparent (Figure 9). A broad distribution (M_w/M_n = 2.4) multi- block copolymer of predominant structure (PMPS-*b*-PI)$_3$ has been demonstrated to form self-supporting films that are optically clear, strong, and flexible [32].They were characterized using both AFM and neutron scattering [49] and despite relatively high polydispersities in both component blocks (respectively 1.64 and 1.34 for PMPS and PI), a regular modulated morphology was observed with average domain repeat units of 18.8 and 18.6 nm at the surface and in the bulk respectively (Figure 10). The regularity was further shown to be entirely consistent with the extended lamella-like structure shown in Figure 11 rather than the thermodynamically less-favored structure within which the chains fold and reverse direction at the coiled PI segments.

The PMMA-*b*-PMPS-*b*-PMMA triblock copolymers prepared by the macroinitiator approach using ATRP [39] were only characterized using differential scanning calorimetry. The glass transition temperature (T_g) of PMPS is usually difficult to observe but within the copolymers it was clearly evident at 125-130 °C. The T_gs

of the PMMA blocks increased with block length in a manner consistent with the variation with chain length for homopolymers of PMMA and were also clearly visible by DSC. The presence of two T_gs provides strong evidence for microphase separation of the blocks.

Films of the POEGMA-*b*-PMPS-*b*-POEGMA series of copolymers synthesized by ATRP [42] were cast on glass, silicon, silver, and gold substrates and were investigated by a number of techniques [47]. The water contact angles at the surfaces of the block copolymers were observed to be directly related to the nature of the underlying substrate; e.g. hydrophilic glass substrate gave a low contact angle (~35º) and a hydrophobic gold substrate gave a relatively high contact angle (~90º) (see Figure 12). Selective delamination from the hydrophilic surfaces (glass and ozone-treated silicon) was observed for those copolymers with a high POEGMA content (weight ratios of POEGMA:PMPS > ~1.3, below this no delamination was observed). I.e. the nature of the substrate (hydrophilic vs. hydrophobic) directly controlled the adhesion of the block copolymer film to the substrate in an aqueous environment. Similar behavior was observed for a corresponding series of POEGMA-*b*-PS-*b*-POEGMA copolymers (in which the central block is polystyrene) of POEGMA:PS weight ratios >~1). Thus the behavior was not intrinsic to polysilane block copolymers. Water contact angles of ~85° were observed for the PHEMA-*b*-PMPS-*b*-PHEMA and PMMA-*b*-PMPS-*b*-PMMA copolymers and a poly methylmethacrylic acid-*block*-polymethyl methacrylate-*block*-polymethyl methacrylic acid copolymer and no delamination was observed upon immersion in water. It was therefore proposed that the presence of POEGMA blocks is a critical factor in addition to appropriate hydrophobic:hydrophilic weight ratios.
The tapping mode AFMs of Figure 13 are examples of the height and phase images of the POEGMA-b-PMPSb-POEGMA films coated on glass. They reveal smooth surfaces with lateral microphase separation. Films of the copolymers coated on gold surfaces (hydrophobic) are similar, as typified by the phase images for both systems shown on the same scale in Figure 13. Despite this the contact angles of water at these surfaces differed considerably. X-ray photoelectron spec-

troscopy, XPS, was used to probe the effects of immersion in water of the hydrophilically unstable films of POEGMA-*b*-PMPS-*b*-POEGMA coated on gold and glass. Prior to immersion, the spectra indicated a slight accumulation of the PMPS on the outer surface of the films. The film coated on gold was unaffected by immersion but that coated on glass indicated a clear shift to a higher POEGMA content at the outer surface. Thus XPS indicated that a rearrangement of the surface morphology took place when the films over glass came into contact with water whereas no rearrangement occurred for films over gold. In contrast, the stable (non-delaminating) films coated on glass have relatively rough, granular surfaces with a micellar-like structure. The thin film cross sections of Figure 14 represent models for the self-organization of the delaminating ABA block copolymers over glass and gold substrates that are based on the above observations.

The amphiphilic block copolymers PHEMA-*b*-PMPS-*b*-PHEMA and POEGMA-*b*-PMPS-*b*-POEGMA have found applications as templates for the patterning of cell growth [51] and the patterning of biomimetic crystallization processes [52]. In the first case the selective delamination of POEGMA-*b*-PMPS-*b*-POEGMA was utilized [51]. Samples were spun-cast onto patterned gold-electrodes (20nm thick, 100-600 μm wide) on a glass substrate. The resulting films were immersed in a cell culture medium for 3 days over which time the copolymer detached from the glass surface but remained on the gold (the delamination was significantly faster using the cell culture medium rather than water) as illustrated schematically in Figure 15. Similar effects were observed for the POEGMA-*b*-PS-*b*-POEGMA samples but in the case of the POEGMA-*b*-PMPS-*b*-POEGMA samples delamination could be monitored by UV-vis spectroscopy by noting the disappearance of the characteristic UV absorption peak due to the PMPS (Figure 15). When the copolymer films were exposed to a cell culture medium in the presence of C2C12 mouse myoblasts (undifferentiated muscle cells) within 24 hours a pattern of aligned myoblasts was visible on the glass lanes between the gold electrodes as a consequence of the delamination of the copolymer (Figure 16). The copolymer film on the gold electrodes remained free of cells as a consequence of the

POEGMA component of the copolymer (poly(ethylene oxide) compounds are resistant to protein adsorption and cell adhesion). It should be noted that this delamination process occurs within films forming a continuous thin films over the glass and gold surfaces. Thus it remains a remarkably simple means of protecting/covering the hydrophobic parts of patterned surfaces through a simple application of a polymer film followed by immersion and rinsing.

The PHEMA-*b*-PMPS-*b*-PHEMA amphiphilic ABA block copolymers were used to generate patterned calcium carbonate films with dimensions of several hundreds of microns using the photolithographic properties of the polysilane component [52]. PHEMA-*b*-PMPS-*b*-PHEMA was spin cast from THF solution onto glass substrates. On this polymer layer continuous films of calcium carbonate, $CaCO_3$, ~ 1μm thick were grown by immersing them in an aqueous $CaCl_2$ solution containing poly(acrylic acid) and allowing CO_2 vapor from $(NH_4)_2CO_3$ to diffuse into these solutions (Figure 17). Surface profilometry showed that the average thickness of the $CaCO_3$ films was~ 1μm. Optical microscopy, FT-IR and SEM all demonstrated that the films were amorphous with few embedded crystalline spherulites. Upon standing, the film crystallized as demonstrated by SEM, FT-IR and Powder X-Ray Diffraction (PXRD). When the polymer films were irradiated with UV light (360 nm) through a mask for 2hrs, the irradiated polymer lanes could be removed selectively by washing with ethanol, resulting in a pattern of polymer lanes 200 μm wide and ~ 30 nm high (as determined by surface profilometry). When these patterned films were subjected to the mineral film formation process, $CaCO_3$ was deposited both on the polymer lanes and on the areas from which the polymer had been removed. However, when the mineral was deposited onto a pre-exposed but undeveloped polymer film, the $CaCO_3$ layer grown on the irradiated lanes could be selectively removed upon immersion of the film into ethanol, resulting in the formation of a patterned $CaCO_3$ film (Figure 18).The non-patterned $CaCO_3$ films could be observed to crystallize within 1 hr by optical microscopy. However the patterned films stayed amorphous for 2-3 hours under ambient conditions and were only completely crystalline after 24 hrs, which is probably due to

the use of ethanol in the patterning procedure, as this is known to stabilize ACC (amorphous calcium carbonate). Subsequently cell culture experiments were performed and the results indicated that the $CaCO_3$ substrates support rat bone marrow stromal cell attachment, proliferation and differentiation into osteoblast and osteoclast-like cells. Moreover, mineral formation by the osteoblast-like cells was favored on the $CaCO_3$ films compared to the developed polymer films. Also, the osteoclast-like cells can degrade the $CaCO_3$ films. Therefore, these patterns of $CaCO_3$ films can be regarded as suitable 2D model substrates for bone cells. In addition, the patterning method presented here is not restricted only to glass substrates unlike the use of patterned SAMs (self-assembled monolayers), where the choice of substrates is limited. In general this method would allow for the photogeneration of patterns of $CaCO_3$ on a variety of substrates, including e.g. conducting polymers, which would be beneficial for electrical stimulation of cells to enhance their proliferation and differentiation.

3.2. Self-Assembly of Polysilane Block Copolymers in Solution

The first self-assembling block copolymers were PS-*b*-PMPS-*b*-PS synthesised by Matyjaszewski and Möller. They observed micellar aggregates by AFM after casting dilute dioxane solutions (a solvent selective for the PS block) of the copolymer. The observed micelles were taken to have internal PMPS cores and were measured at 25-30nm in diameter [48]. The first self-assembling amphiphilic polysilane block copolymers to be investigated was the PMPS-PEO multi-block copolymer with normal distribution PMPS blocks and uniform low polydispersity PEO blocks. After dialysis aqueous dispersions of this copolymer formed micellar as well as vesicular structures [53] as shown in Figure 19. Encapsulation of the water soluble 5-carboxyfluoroscein dye confirmed the formation of vesicles. A pressure-area isotherm was recorded for a monolayer of the copolymer at the air-

water interface to investigate the likely orientation of chains in the vesicle walls. A lift-off area of 30 nm^2 $molecule^{-1}$ corresponding to the approximate cross sectional area of three PMPS chains oriented perpendicular to the air-water interface were observed. More detailed studies [54] of the surface viscoelastic properties of the spread films at the air-water interface have revealed complex relaxation processes that follow none of the simple models that might be expected. This was attributed to the rigid nature of the polysilane blocks. The UV-vis spectra of the aqueous dispersions display a σ-σ^* transition associated with a λ_{max} = 342 nm compared to molecularly dissolved PMPS with λ_{max} = 337 to 340 nm, indicating that within the aggregates the polysilane segments were more extended than in solution. Based on these observations a structural model of the vesicles could be constructed (Figure 19).

The aggregation of the PMPS-PEO copolymers in solution and dispersion was furthered probed using fluorescence spectroscopy. A small red shift in the fluorescent emission maximum was observed on increasing the water content, attributable to more effective energy transfer from shorter to longer PMPS segments. This indicated that higher water contents induced the alignment of PMPS segments. Absorption spectra showed similar trends. Below 40% water content the block copolymer was molecularly dissolved as evidenced by TEM and dynamic light scattering. However, from 40% to 80% water content, micellar fibers with diameters of 20 nm and up to several microns in length were observed. TEM images of samples both unstained and stained with uranyl acetate are shown in Figures 20a-c. The unstained sample highlights the hydrophobic PMPS segments and the stained sample also shows the polar PEO segments as a protective hydrophilic sheath around the core of PMPS as depicted in the schematic of Figure 20d. At water concentrations above 80%, both right- and left-handed helical aggregates were observed. These superstructures had lengths of 1—2 μm, widths up to 0.2 m, and a pitch of approximately 0.15 m (Figure 21). The helicity of the aggregates was attributed to the known helical conformation of the polysilane segments [20, 21] arising form the close-packing of helical segments of the same screw-sense.

This was in analogy to the close packing of the rigid helical poly(isocyanide) segments in polystyrene and peptide based poly(isocyanide) block copolymers.

The masked disilene procedure was used by Sakurai and co-workers to synthesize two samples of diblock copolymers of 1,1-dimethyl-2,2-dihexylsilane (MHS) and 2-(trimethylsilyloxy)ethyl methacrylate, which differed only in the relative lengths of their blocks. Hydrolysis of the trimethylsilyl protecting groups gave the corresponding amphiphilic diblock copolymers, poly(1,1-dimethyl-2,2- dihexyldisilene)-b-poly(2-hydroxyethyl methacrylate) (PMH S-b-PHEMA), depicted in Figure 22 [33]. In the solid state at room temperature, PMHS has a λ_{max} at 334 nm in which it takes on an ordered conformation (originally thought to be *trans* but most probably helical) but in toluene has a λ_{max} of 307 nm (resulting from a disordered conformation). The PMHS-*b*-PHEMA copolymer (copolymer 1) in methanol exhibits absorption with a λ_{max} at 334 nm so it was concluded that the PMHS blocks existed in a hydrophobic micellar core as a solid surrounded by the hydrophilic PHEMA blocks. In toluene solution, copolymer 2, with relatively shorter HEMA blocks, exhibited a λ_{max} of 307 nm. Thus, the PMHS blocks exist either in a corona or are molecularly dissolved. In addition, copolymer 1 showed solvatochromism related to the change between micelles and unimers. Copolymer 1 forms kinetically frozen micelles as the component polysilane block has a glass transition temperature (T_g) higher than room temperature so the morphology can be observed directly using AFM operating in the tapping mode. A cast solid film on mica-coated from a methanol solution indicated ellipsoidal micellar structures with a size of 50-60 nm in agreement with the observations of static light scattering experiments (Figure 23).

Poly(1,1-dimethyl-2,2-dihexyldisilene)-*block*-poly (methacrylic acid) (PHMS -*b*-PMAA) with a PMHS:PMAA molar monomer unit ratio of 1:20 was also prepared by a sequential anionic polymerization of ‘masked’ disilenes and trimethylsilyl methacrylate, followed by hydrolysis of the trimethylsilyl protecting group [34]. PMHS-*b*-PMAA was soluble in water and self-assembled to form polymer micelles with an average diameter of 170 nm in water at a concentration of 0.2 g L-1

at 25 °C.

Subsequently methacrylic acid block was reacted with 2,2-(ethylenedioxy)diethylamine to form shell cross-linked micelles (SCM) (Figure 24). ^{1}H-NMR signals from the PHMS core could not be detected in D_2O solution because of very long relaxation times arising from the solid core, however, upon the addition of an excess of THF-d8 to the solution, signals from the core were observed as the PMHS blocks became solvated. Solid state CP-MAS ^{29}Si NMR demonstrated the presence of two signals at -27.6 and -35.7 ppm, assignable to dihexylsilylene and dimethylsilylene units, respectively. DLS studies indicated the intensity-averaged diameter of the particles to be 160 nm with mono-dispersed spheres, consistent with the size of the micelles of the parent PMHS-*b*-PMAA**,** though slightly shrunken. AFM images revealed spherical particles of about 50 nm diameter in the dry state.

The polysilane core part within the shell cross-linked micelles was photodegraded by UV irradiation (≥ 280 nm) and dialysis against water produced nanometer-sized hollow particles (Figure 25) [35]. In the UV absorption spectra, a continuous blue shift in the absorption maximum was observed during photoirradiation confirming degradation of the polysilane core. Subsequently 5,6-carboxyfluorescein (CF) was encapsulated into the nanometer-sized hollow particles prepared by a similar procedure; prolonged dialysis led to the release of the dye from the particles. A further application of these SCMs involved the reduction of $HAuCl_4$ with the polysilane core of the micelles [55]. Polysilanes have relatively low oxidation potentials and consequently are able to reduce certain metal ions with the Si-Si bonds undergoing oxidation to Si-O bonds. In this manner gold-nanoparticles of 12 ± 5.7nm in diameter were produced in the cores of the SCMs with diameters of 25 ± 5.7nm. The SCM Au nanoparticles were characterized by TEM and UV-vis spectroscopy. In a similar manner the polysilane micelles were used to reduce $PdCl_4^-$ to give SCM Pd nanoparticles of 20 ± 10.7nm diameter [56]. The SCM-Pd nanoparticles were subsequently shown to be effective catalyst for alkene hydrogenation and in Heck reactions. The polysilane-PMA block copolymers prepared

in this study were further utilized in stabilizing silica nanoparticles through chemical attachment to aminopropyl surface groups.

To complement the aggregation studies of the multi-block PMPS-PEO polymers, the self-assembly of the amphiphilic triblock copolymers, PHEMA-*b*-PMPS-*b*-PHEMA and POEGMA-*b*-PMPS-*b*-POEGMA were investigated [42]. Series of each of the block copolymers, prepared using the ATRP macroinitiator approach, were studied using TEM and dynamic light scattering. In the case of the PHEMA-*b*-PMPS-*b*-PHEMA copolymers in aqueous dispersion, only micellar aggregates 10-20 nm in diameter were observed (Figure 26a). In contrast, aqueous dispersions of POEGMA-*b*-PMPS-*b*-POEGMA contained some large spherical aggregates with diameters of between 300 and 1000 μm among a lot of micellar material of diameter 15—30 nm (Figure 26b). Silicon having a significantly greater electron capture cross-section than carbon, the dark areas in the centers of the larger aggregates are taken to be silicon-containing regions. In some cases, sheet-like aggregates were formed (Figure 26c) and electron diffraction patterns (Figure 26d), revealed these to have a hexagonal close-packed internal structure. PMPS is usually described as being amorphous but has been shown to possess 10% crystallinity and to have a diffraction pattern of near hexagonal symmetry for a mesophase [58]. However, the high level of organization within the block copolymer indicates a bilayer with a smectic-like arrangement of the PMPS chains that is not dissimilar to observations of amphiphilic polythiophenes in aqueous dispersion [59]. The degradation of several of the polysilane aggregates upon exposure to UV light (λ_{max} = 254 nm) was demonstrated by monitoring the drop in the intensity of the UV absorption band at 334 nm (Figure 27). All aggregates were shown to degrade with only slight variations in rate. Such degradation shows that polysilane block copolymer aggregates hold promise as light stimuli-responsive materials. Studies are currently underway in our group to encapsulate hydrophobic materials in the polysilane hydrophobic cores of these micelles and control release of the encapsulated materials through exposure to UV light (Figure 28).

4. Conclusions

A number of approaches to the synthesis of polysilane copolymers exist and the most promising have led to the synthesis of a number of polysilane block copolymer structures. Arguably the most intriguing of these are the classic amphiphilic block copolymers containing hydrophobic polysilane components and hydrophilic vinyl polymer blocks. Thin films of polysilane block copolymers have been demonstrated to adopt microphase separated structures with cylindrical or lamellar morphologies predominating. A number of polysilane block copolymers have been shown to form aggregates in aqueous solutions, predominantly micelles but vesicles and bilayers are also evident. The latter structures arising most likely as a result of the rod-like structure of the polysilane components. Despite interest in the optical and electronic properties of polysilanes the most interesting applications of their block copolymers have been in using their photolability as a means to pattern thin films (e.g. for controlled crystallization) or generate unique aggregate structures (e.g. hollow shell-cross-linked micelles). This might not be considered surprising as this is an almost unique feature of polysilane materials; their ability to undergo photodegradation under non-extreme conditions. In contrast many of their optical and electronic properties are matched and/or exceeded by the vast array of π-conjugated polymers and copolymers that have been synthesized and studied over the past two decades. It is likely that the any future applications and interest in polysilane block copolymers will reside in the coupling of this photolability with other properties resulting from the complementary block.

References

[1] Miller RD, Michl J (1989) ChemRev 89:1359 and references therein

[2] Shieh YT, Hsu TM, Sawan SP (1996) J Appl Polym Sci 62:1723

[3] Keppler RG, Zeigler JM, Harrah LA, Kurtz SR (1987) Phys Revs B35:2818

[4] Samuel LM, Sanda PN, Miller RD (1989) ChemPhysLett 159:227

[5] Suzuki H, Hoshino S, Furukawa K, Ebata K, Yuan CH, Bleyl I (2000) Polym Adv Technol 11:460

[6] Hasegawa T, Iwasa Y, Koda T, Kishida H, Tokura Y, Wada S, Tashiro H, Tachibana H, Matsumoto M, Miller RD (1995) Synth Met 71:1679

[7] Kishida ZH, Hasegawa T, Iwasa Y, Koda T, Tokura Y, Tachibana H, Matsumoto M,SWada, Lay IT,Tashiro H (1994) Phys Revs B50:7786

[8] Yajima S, Hasegawa Y, Hayashi J, Iiinura HJ (1978) J Mater Sci 13:2569

[9] Yajima S, Hayashi J, Omori M (1975) Chem Lett 931

[10] Peinado C, Alonso A, Catalina F, Schnabel W (2000) Macromol Chem Phys 201:1156

[11] Yacgi Y, Schnabel W (1992) Macromol Chem Macromol Symp 60:133

[12] Miller RD, Walraff G, Clecal N, Sooriyakurnaran R, Michl J, Karatsu T, McKinley AI, Klingensmith KA, Downing J (1989) J Polym Eng Sci 29:882

[13] Hamley IW, The Physics of Block Copolymers, Oxford University Press:Oxford, 1998

[14] Discher BM, Hammer DA, Bates FS, Discher DE (2000) Curr Opin Colloid Interface Sci 5:125-131

[15] Zhang L, Eisenberg A (1995) Science 268:1728-1731

[16] Won YY, Davis HT, Bates FS (1999) Science 283:960-963

[17] Kataoka K, Harada A, Nagasaki Y (2001)Adv Drug Deliv Rev 47:113-131 (b) Allen C, Maysinger D, Eisenberg A (1999) Colloids Surf B:Biointerfaces 16:3–27 (c) Kakizawa Y, Kataoka K (2002) Adv Drug Deliv Rev 54:203-222

[18] Caruso F, Caruso RA, Mohwald H (1998) Science 282:1111-1114

[19] (a) Liu J, Sheina E, Kowalewski T, McCullough RD (2002) Angew Chem Int Ed 41:329-332 (b) Jenekhe SA, Chen XL (1999) Science 283:372-375, (c) Jenekhe SA, Chen X Science (1998) 279:1903-1907 (d) Chen XL, Jenekhe SA (2000) Macromolecules 33:4610-4612 (e) de Boer B, Stalmach U, van Hutten PF, Melzer C, Krasnikov VV, Hadziioannou G (2001) Polymer 42:9097-9109 (f) van Hutten PF, Krasnikov VV, Hadziioannou G (2001) Synthetic Metals 122:83-86 (g) Stalmach U, de Boer B, Videlot C, van Hutten PF, Hadziioannou G (2000) J Am Chem Soc 122:5464-5472 (h) Widawski G, Rawiso M, Francois B (1994) Nature 369:387-389

[20] Fujiki M (2001) Macromol Rapid Commun 22:539 and references therein

[21] Fujiki M, Koe J (2000). In: Jones RG, Ando W, Chojnowski J (eds) Silicon-Based Polymer: The Science and Technology of Their Synthesis and Applications, Kluwer Academic Publishers, Dordrecht

[22] Mark JE, Allcock HR, West R (1992) Inorganic Polymers. Prentice-Hall, New Jersey

[23] Cypryk M, Chrusciel J, Fossum E, Matyjaszewski K (1993) Makromol Chem Macromol Symp 73:167

[24] Sakamoto K, Obata K, Hirata H, Nakajima M, Sakurai H (1989) J Am Chem Soc 111:7641

[25] Aitken C, Harrod JF, Samuel E (1985) J Organomet Chem 279:C11

[26] Jones RG, Ando W, Chojnowski J (2000) Silicon-Based Polymers: The Science and Technology of their Synthesis and Applications. Kluwer Academic Publishers, Dordrecht

[27] (a) Jones RG, Budnick U, Holder SJ, Wong WKC (1996) Macromolecules 29:8036 (b) Jones RG, Wong WKC, Holder SJ (1998) Organometallics 17:59 (c) Holder SJ, Achilleos M, Jones RG (2005)Macromolecules 38:1633-1639

[28] (a) West R, Wolff AR, Peterson DJ (1986) J Radiat Cur 13:35 (b) Yucesan D, Hostoygar H, Denizligil S, Yacgi Y (1994) Angew Makromol Chem 221:207 (c) Yacgi Y, Krninek I, Schnabel W (1993) Polymer 34:426 (d) Wolff A, West R (1987) Appl Organomet Chem 1:7
[29] Demoustier-Champagne S, de Mahieu AF, Devaux J, Fayt R, Teyssie Ph (1993) J Polym Sci 31:2009-2014
[30] (a) Demoustier-Champagne S, Canivet I, Devaux J, Jerome R (1997) J Polym Sci Part A:Polym Chem 35:1939-1948 (c) Schwegler LA, Sheiko SS, Moller M, Fossum E, Matyjaszewski K (1999) Macromolecules 32:5901-5904
[31] Lutsen L, Jones RG (1998) Polym Int 46:3-10
[32] Hiorns RC, Holder SJ, Schué F, Jones RG (2001) Polym Int 50:1016
[33] Sanji T, Kitayama F, Sakurai H (1999) Macromolecules 32:5718
[34] Sanji T, Nakatsuka Y, Kitiyama F, Sakurai H (1999) J Chem Soc Chem Commun 2201
[35] Sanji T, Nakatsuka Y, Ohnishi S, Sakurai H (2000) Macromolecules 33:8524
[36] (a) Fossum E, Love JA, Matyjaszewski K (1995) J Organomet Chem 499:253 (b) Fossum E, Matyjaszewski K (1995). In: Jones RG (ed) Silicon-Containing Polymers, Royal Society of Chemistry, Cambridge
[37] Matyjasewski K, (2000) Controlled/"Living" Radical Polymerization:Progress in ATRP, NMR and RAFT. American Chemical Society, Washington,DC,
[38] (a) Kato M, Kamigaito M, Sawamoto M, Higashimura T (1995) Macromolecules 28:1721-1723 (b) Wang S, Matyjaszewski K (1995) Macromolecules 28:7901-7910 (c) Percec V, Barboiu B(1995) Macromolecules 28:7970-7972
[39] Anderson RM, Holder SJ, Jones RG, Rossi NAA (2003) Polym Internat 53:465
[40] Jones RG, Holder SJ (1997) Macromol Chem Phys 198:3571
[41] Rossi NAA, Jones RG, Holder SJ (2003) J Pol Sci PartA:Polym Chem 41:30
[42] Holder SJ, Rossi NAA, Yeoh C-T, Durand GG, Boerakker MJ, Sommerdijk NAJM (2003) J Mater Chem 13:2771
[43] Hamley IW, The Physics of Block Copolymers, Oxford University Press:Oxford, 1998
[44] (a) Bates FS, Frederickson GH (1990) Ann Rev Phys Chem 41:525 (b) Thomas EL, Lescanec RL (1994) Philos Trans R Soc London Ser A 348:149-166 (c) Klok HA, Lecommandoux S (2001) Adv Mater 13:1217
[45] (a) Mansky P, Harrison CK, Chaikin PM, Register RA, Yao N (1996) Appl Phys Lett 68:2586 (b) Park M, Harrison CK, Chaikin PM, Register RA, Adamson DA (1997) Science 276:1401
[46] (a) Fink Y, Urbas AM, Bawendi MG, Joannopoulos JD, Thomas EL, (1999) J Lightwave Techn 17:1963 (b) Urbas AM, FinkY, Thomas EL (**1999**) Macromolecules 32:4748 (c) Urbas AM, Sharp R, Fink Y, Thomas EL, Xenidou M, Fetters LJ (2000) Adv Mater 12:812
[47] (a) Liu GJ, Ding JF, Hashimoto T, Kimishima K, Winnik FM, Nigam S (1999) Chem Mater 11:2233 (b) Nardin C, Winterhalter M, Meier W (2000) Langmuir 16:7708
[48] Fossum E, Matyjaszewski K, Sheiko SS, Möller M Macromolecules (1997) 30:1765-1767
[49] Hiorns RC, Martinez H (2003) Synth Met 139:463
[50] Popescu DC, Rossi NAA, Yeoh C-T, Durand GG, Wouters D, Leclère PELG, Thüne P, Holder SJ, Sommerdijk NAJM (2004) Macromolecules 37:3431-3437
[51] Popescu DC, Lems R, Rossi NAA, Yeoh C-T, Holder SJ, Bouten CVC, Sommerdijk NAJM (2005) Adv Mater 17:2324-2329
[52] Popescu DC, van Leeuwen ENM, Rossi NAA, Holder SJ, Jansen JA, Sommerdijk NAJM (2006) Angew Chem Int Ed 45:1762-1767
[53] (a) Holder SJ, Hiorns RC, Williams SJ, Sommerdijk NAJM, Jones RG, Nolte RJM (1998) Chem Comm 1445 (b) Sommerdijk NAJM, Holder SJ, Hiorns RC, Jones RG, Nolte RJM (2000) Macromolecules 33:8289
[54] Milling AJ, Richards RW, Hiorns RC, Jones RG (2000) Macromolecules 33:2651-2661

[55] Sanji T, Ogawa Y, Nakatsuka Y, Tanaka M, Sakurai H (2003) Chemistry Letters 32:980-981
[56] Sakurai H (2006) Proc Jap Acad Ser B: Phys Bio Sci 82:257-269
[57] Sanji T, Nakatsuka Y, Sakurai F (2005) Polym J 37:1-6
[58] Demoustier-Champagne S, Jonas A, Devaux J (1997) J Poly Sci B:Polym Phys 35:1727-1736
[59] Brustolin F, Goldoni F, Meijer EW, Sommerdijk NAJM (2002) Macromolecules 35:1054-1059
[60] Sanji T, Takase K, Sakurai H (2001) J Am Chem Soc 123:12690-12691

Figure Legends

Fig. 1. Polysilane syntheses: the four main techniques

Fig. 2. Typical synthesis of a polystyrene-block-polysilane-block-polystyrene by a polymer coupling reaction

Fig. 3. Synthesis of a polymethylphenylsilane-poly(ethylene oxide) multi-block copolymer

Fig. 4. Approaches to the synthesis of polysilane block copolymers by living polymerization techniques: (a) via anionic polymerization of masked disilenes; (b) via anionic ring-opening polymerization of cyclotetrasilanes

Fig. 5. Synthesis of polystyrene-*block*-polymethylphenylsilane-*block*-polystyrene by a TEMPO mediated macroinitiator approach

Fig. 6. Synthesis of various polymethylphenylsilane block copolymers by an ATRP based macro-initiator approach.

Fig. 7. ATRP of MMA from a Br-PMPS-Br macro-initiator: (a) SEC traces showing growth of a PMMA chain; (b) kinetic plots for the polymerisation of MMA demonstrating living nature eof polymerization

Fig. 8. TEM picture of a thin section of a film of a PMPS-b-PS copolymer prepared by slow evaporation from THF. Scale bar = 150 nm. Reproduced with permission from [48], Fossum et al., Macromolecules (1997) 30:1765-1767. ©American Chemical Society

Fig. 9. SFM micrographs of a thick film of polystyrene-block-PMPS with Mn = 18,700 and 9,000 and overall polydispersity Mw/Mn = 1.22 (a) before and (b) after degradation with 360 nm light. Reproduced with permission from [48], Fossum et al., Macromolecules (1997) 30:1765-1767. © American Chemical Society

Fig. 10. (a) Representative AFM image of a PMPS-b-PI surface (root mean square roughness over imaged area, 0.071 nm). (b) Profile of PMPS-b-PI surface along line drawn in (a). Maximum distance between domain peaks: 22.0 nm; minimum distance: 16.8 nm. Reproduced from [49], Hiorns and Martinez (2003) Synth Met 139:463

Fig. 11. Tentative, idealised, sectional representation of microphase separation and organization in a PMPS-b-PI film.

Fig. 12. Water contact angles (□) of different substrates. The block copolymer films of POEGMA-b-PMPS-b-POEGMA and POEGMA-b-PS-b-POEGMA selectively delaminate only from the substrates with a hydrophilic surface upon immersion in H2O. Reproduced with permission from [50] Popescu et al., (2004) Macromolecules 37:3431-3437. © American Chemical Society

Fig. 13. Tapping mode AFM phase images of films of POEGMA-b-PMPS-b-POEGMA spin-coated on a gold and on a glass substrate. Reproduced with permission from [50] Popescu et al., (2004) Macromolecules 37:3431-3437. © American Chemical Society

Fig. 14. Postulated models for the self-organization of the delaminating POEGMA-b-PMPS-b-POEGMA and POEGMA-b-PS-b-POEGMA block copolymers over gold and glass substrates (cross section) [50].

Fig. 15. Selective delamination process of POEGMA-PMPS-POEGMA films from glass. A) UV spectra of POEGMA-PMPS-POEGMA films deposited on glass, as spincoated (a - black), after 3 days exposure to H_2O (b – green), after 5 days exposure to H_2O (c – red) and after 3 days exposure to C2C12 cell culture medium (d – blue). B) Cross sectional schematics of the process of selective delamination upon exposure to cell culture medium and cell seeding on the substrates resulting in the formation of a pattern of non –adhesive copolymer-coated gold lanes next to clean glass lanes where the cells can attach. C) Schematic gold electrode arrangements on glass surface. Reproduced with permission from Popescu et al. (2005) Advanced Materials 17:2324-2329. © Wiley-VCH Verlag GmbH & Co.

Fig. 16. A, B) Optical micrographs of C2C12 mouse myoblasts attached to the glass lanes where the POEGMA-PMPS-POEGMA film has delaminated. After A) 24 hrs at a high cell seeding density, B) 8 days, after differentiation into myotubes. Scale bars: 100 μm. (dark gray – gold lanes; light gray – glass lanes). C) SEM image of the aligned C2C12 myotubes (13 days after seeding on the substrates). The arrows indicate the direction of the glass lanes. Reproduced with permission from [51], Popescu et al. (2005) Advanced Materials 17:2324-2329. © Wiley-VCH Verlag GmbH & Co.

Fig. 17. Schematic representation of (a) a 2D model substrate consisting of alternating lanes of mineral (CaCO3) and non-mineralized lanes and (b) of the experimental procedure for the generation of patterns of CaCO3. Dimensions are not to scale. Reproduced with permission from [52] Popescu et al., (2006) Angew Chem Int Ed 45:1762-1767. © Wiley-VCH Verlag GmbH & Co.

Fig. 18. Optical micrographs under cross-polarized light of (a) a pattern of CaCO3 discrete crystals, (b) a pattern of CaCO3 film, grown on patterned thin films of PHEMA-b-PMPS-b-PHEMA. Reproduced with permission from [52] Popescu et al., (2006) Angew Chem Int Ed 45:1762-1767. © Wiley-VCH Verlag GmbH & Co.

Fig. 19. (a, b) TEM images of vesicle dispersions of PMPSn-PEOm showing (a) a replica of intact (freeze fracturing) and (b) collapsed vesicles (platinum shadowing); bars represent 200 nm. (c) Schematic representation of the proposed structure of the vesicles showing the hydrophobic PMPS interior (black) shielded from the aqueous phase by the hydrophilic PEO layers (gray). Reproduced with permission from [53b], Sommerdijk et al. (2000) Macromolecules 33:8289. © American Chemical Society

Fig. 20. Micellar fibers of PMPSnPEOm in mixtures of THF and water (25/75 by volume). TEM images (a) visualizing the polysilane core of micellar fibers (unstained, bar represents 250 nm); (b) revealing the PEO shell using uranyl acetate staining, (c) showing an example of the bulges found for many of these fibers. (d) Schematic representation of the structure of the micellar fibers showing the PMPS core and the PEO shell. Reproduced with permission from [53b], Sommerdijk et al. (2000) Macromolecules 33:8289. © American Chemical Society

Fig. 21. Helical aggregates of PMPSnPEOm found in a water/THF mixture of 90/10 (v/v). (a) TEM image (unstained, bar represents 250 nm) of a right-handed helix and (b) SEM image (uncoated, bar represents 250 nm) of a left-handed helix. (c) Schematic representation of the forma-

tion of a superhelix from the coiling of two helical stands. Reproduced with permission from [53b], Sommerdijk et al. (2000) Macromolecules 33:8289. © American Chemical Society

Fig. 22. Synthesis of amphiphilic diblock copolymers of poly(1,1-dimethyl-2,2-dihexyldisilene)-b-poly(2-hydroxyethyl methacrylate). Reproduced with permission from [33] Sanji et al. (1999) Macromolecules 32:5718. © American Chemical Society

Fig. 23. Tapping mode AFM images and vertical profile of poly(1,1-dimethyl-2,2- dihexyldisilene)-b-poly(2-hydroxyethyl methacrylate) in the solid film on mica coated from a methanol solution (0.043 g/L). Reproduced with permission from [33] Sanji et al. (1999) Macromolecules 32:5718. © American Chemical Society

Fig. 24. Schematic illustration of the synthetic pathway for hollow square particles derived from polysilane shell cross-linked micelles templates. Reproduced with permission from [35] Sanji et al. (2000) Macromolecules 33:8524. © American Chemical Society

Fig.25. Hollow particles prepared from SCMs of poly(1,1-dimethyl-2,2-dihexyldisilene)-b-poly(methacrylic acid), (a) AFM image on Pyrex glass plate with operating in the contact mode, (b) vertical profile of the hollow particle shown in part (a), and (c) in the tapping mode under THF wet conditions. Reproduced with permission from [35] Sanji et al. (2000) Macromolecules 33:8524. © American Chemical Society

Fig. 26. TEM images of (A) PHEMA-b-PMPS-b-PHEMA micelles, (B) POEGMA-b-PMPS-b-POEGMA large spherical aggregates (C) POEGMA-b-PMPS-b-POEGMA sheet structures with inset (D) a diffraction pattern demonstrating hexagonal packing. Reproduced from [42], Holder et al. (2003) J Mater Chem 13:2771. © The Royal Society of Chemistry

Fig. 27. Irradiation from 180–600 nm: (a) UV-Vis spectra recorded at 60 min intervals for the degradation of PHEMA-b-PMPS-b-PHEMA aggregates; (b) a plot of A/A0 x 100% at □max versus irradiation time for various copolymer aggregates.

Fig. 28. Schematic illustrating proposed mechanism for the light induced release of encapsulated materials from polysilane micelle cores.

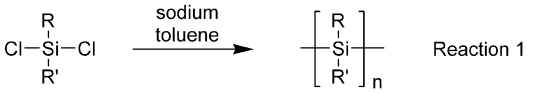

Reaction 1

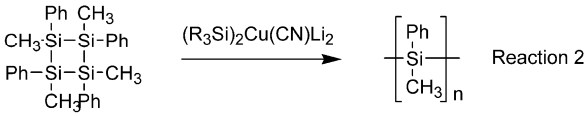

Reaction 2

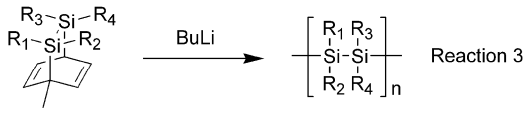

Reaction 3

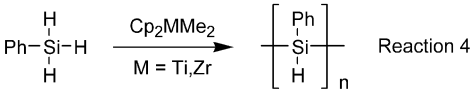

Reaction 4

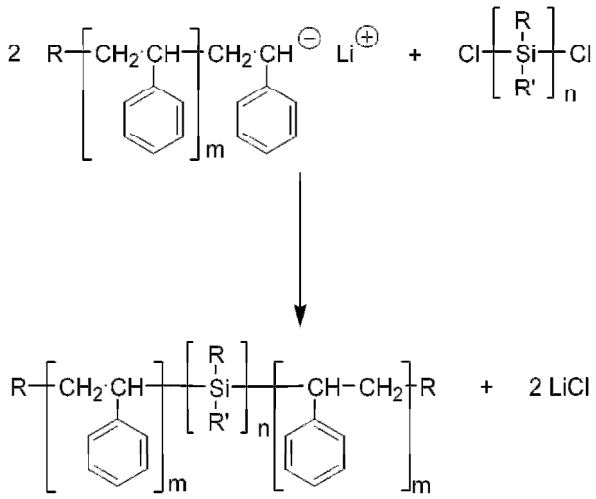

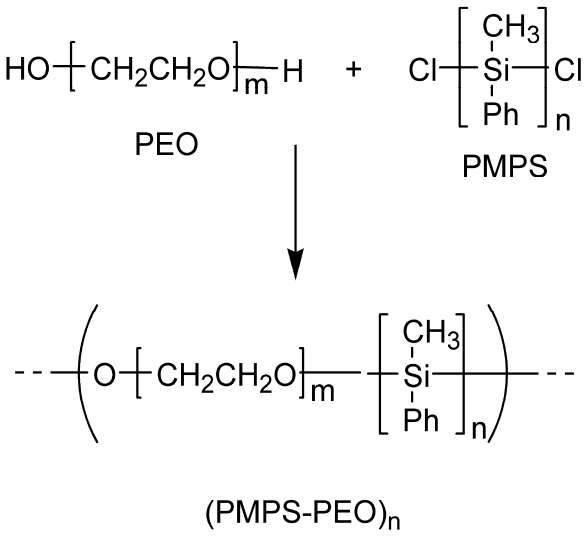

$(PMPS\text{-}PEO)_n$

(a)

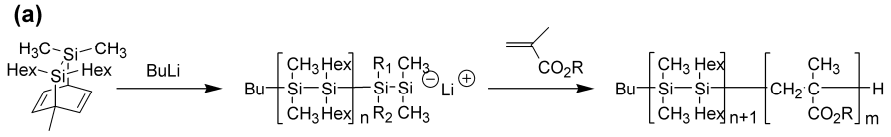

PHMS-*b*-PMMA R = CH_3
PHMS-*b*-PTMSEMA R = $CH_2CH_2OSi(CH_3)_3$
PHMS-*b*-PTMSMA R = $Si(CH_3)_3$

(b)

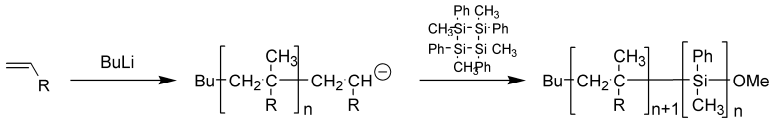

PMP-*b*-PS R = Ph
PMPS-*b*-PI R = $CH{=}CH_2$

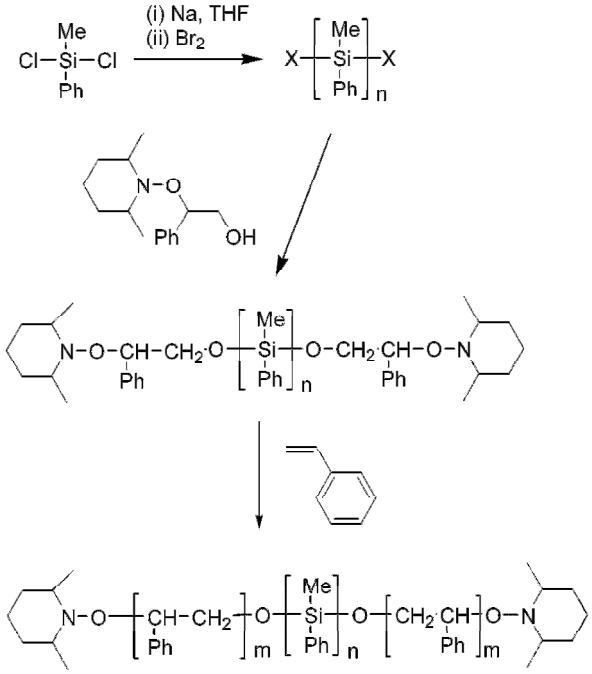
(i) Na, THF
(ii) Br2
Me
Cl–Si–Cl
Ph
X–Si–X
n
N–O
Ph
OH
O–CH2–CH–O–N
m

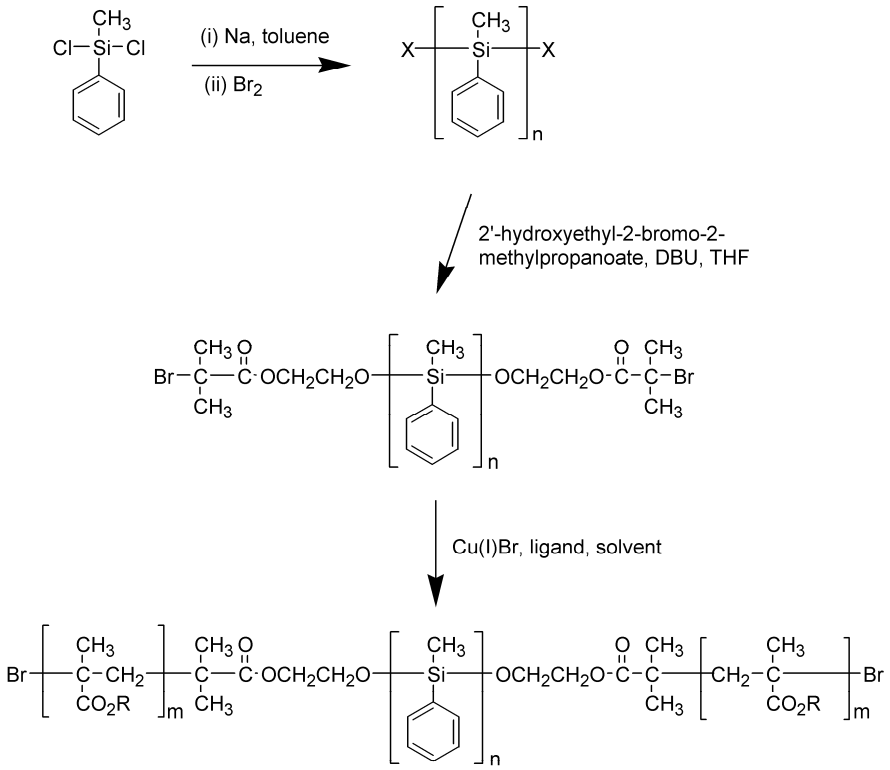

R = -CH_3 **PMMA-PMPS-PMMA**
R = -$(CH_2CH_2O)_{4.5}$-CH_3 **POEGMA-PMPS-POEGMA**
R = -CH_2CH_2OH **PHEMA-PMPS-PHEMA**

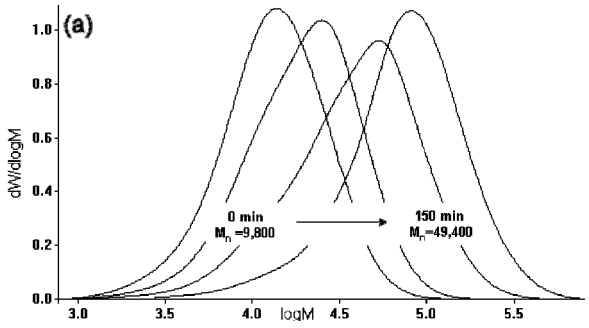
(a)
dW/dlogM
1.0
0.8
0.6
0.4
0.2
0.0
0 min
M_n =9,800
150 min
M_n=49,400
3.0
3.5
4.0
logM
4.5
5.0
5.5

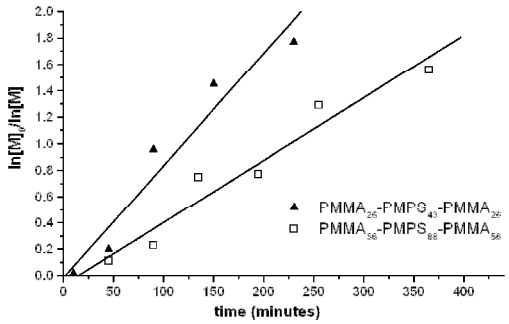
ln[M]$_0$/ln[M]
2.0
1.8
1.6
1.4
1.2
1.0
0.8
0.6
0.4
0.2
0.0
0
50
100
150
200
250
300
350
400
time (minutes)
PMMA$_{26}$-PMPS$_{43}$-PMMA$_{26}$
PMMA$_{56}$-PMPS$_{88}$-PMMA$_{56}$

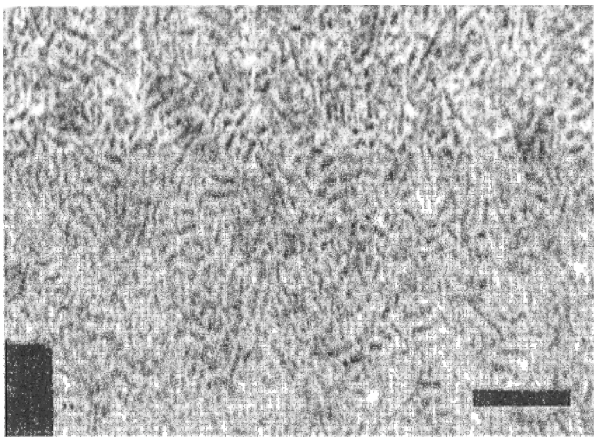

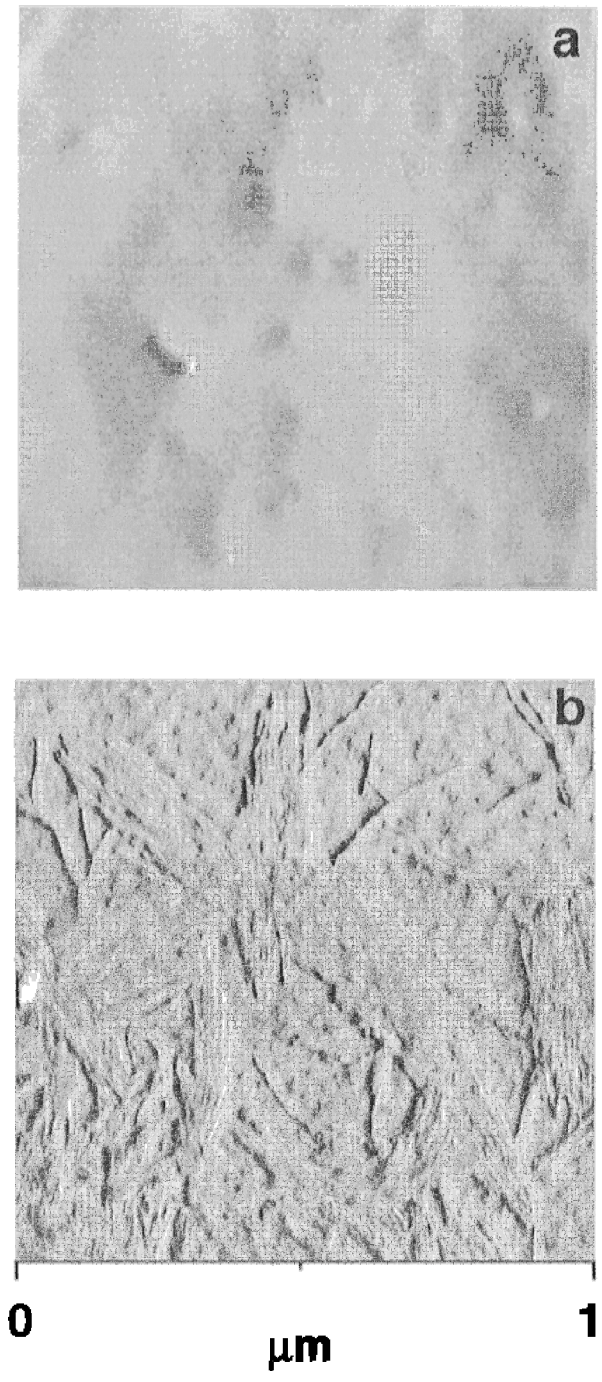
a
b
0
1
μm

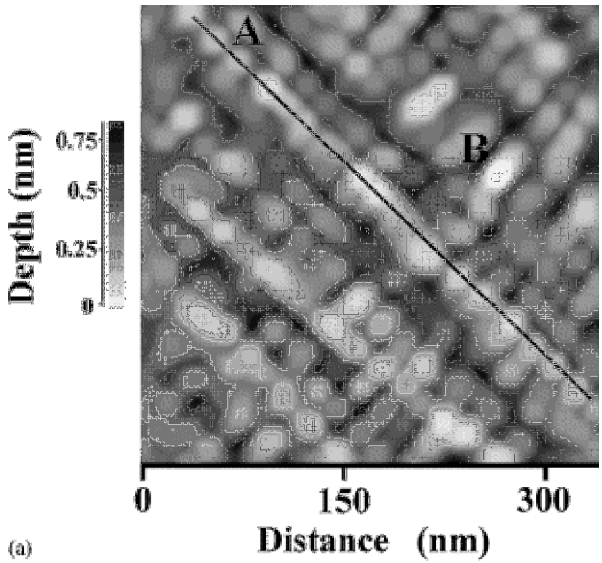
A
B
Depth (nm)
0.75
0.5
0.25
0
0
150
300
Distance (nm)

(a)

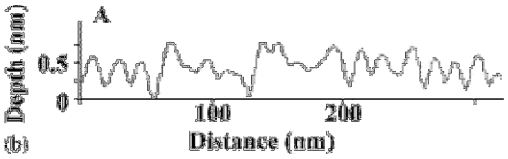
A
Depth (nm)
0.5
0
100
200
Distance (nm)

(b)

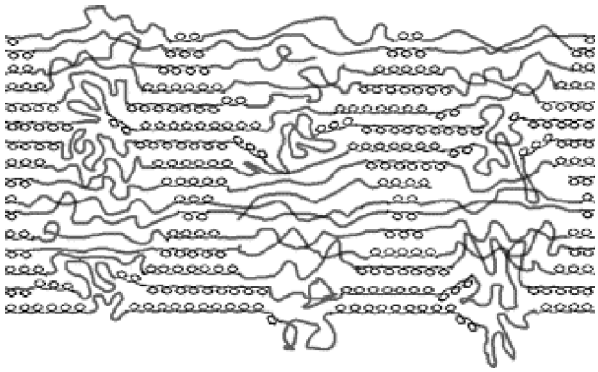

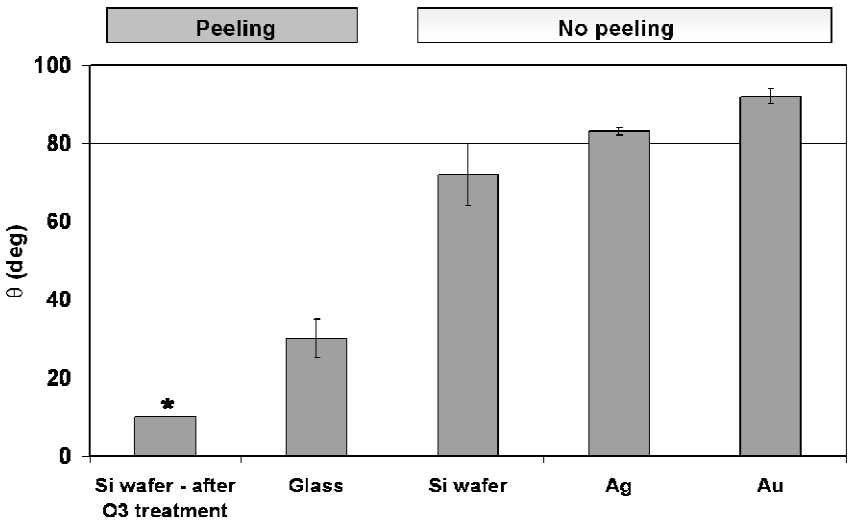

* Very hydrophilic surface; θ<10° (difficult to measure accurate values using the sessile drop method)

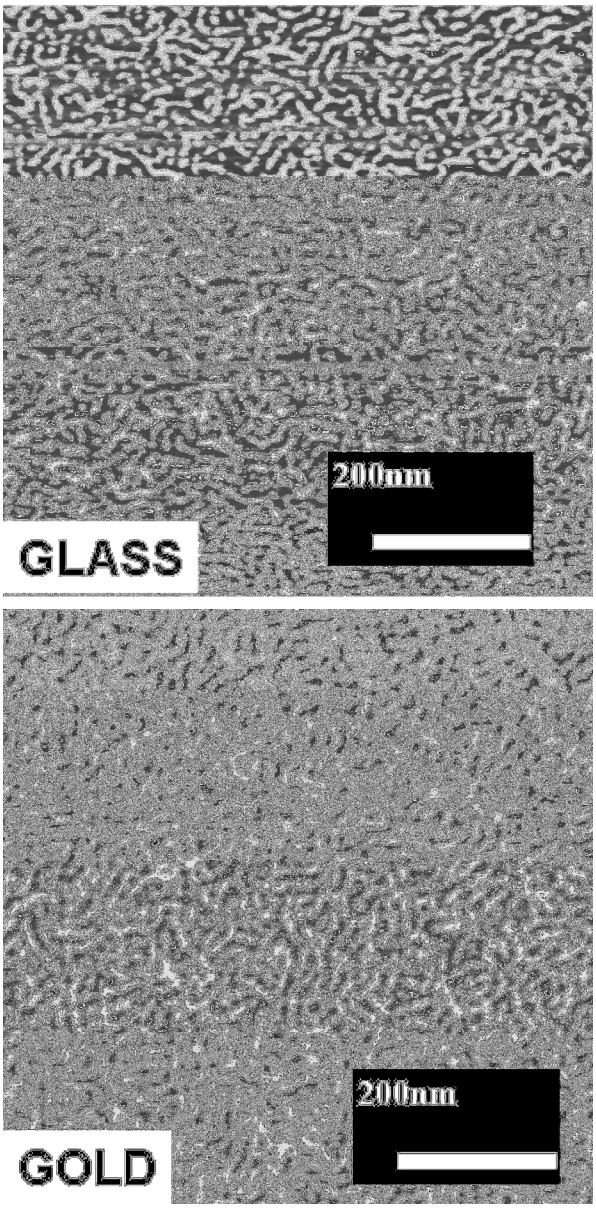
200nm
GLASS
200nm
GOLD

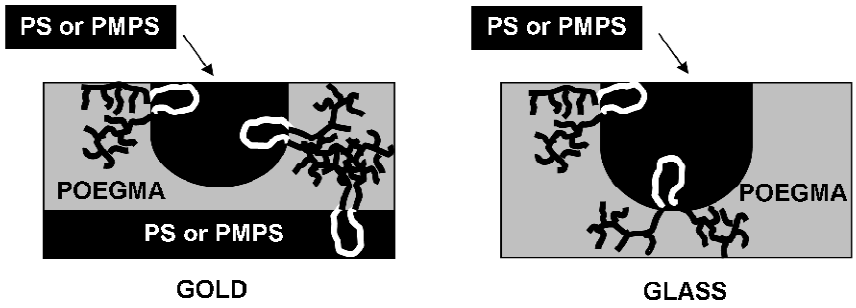
PS or PMPS
POEGMA
PS or PMPS
GOLD
PS or PMPS
POEGMA
GLASS

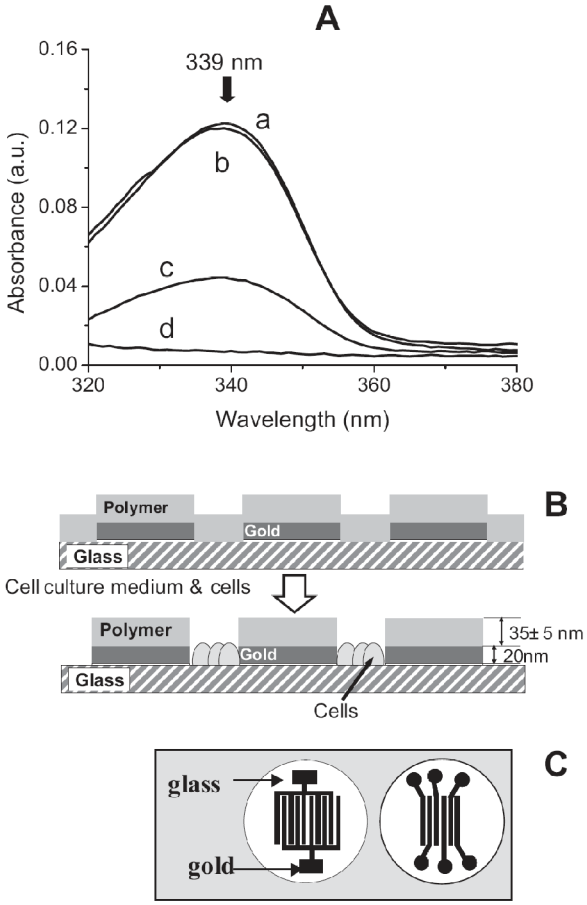
A
339 nm
a
b
c
d
Absorbance (a.u.)
Wavelength (nm)
0.16
0.12
0.08
0.04
0.00
320
340
360
380
B
Polymer
Gold
Glass
Cell culture medium & cells
35± 5 nm
20nm
Cells
C
glass
gold

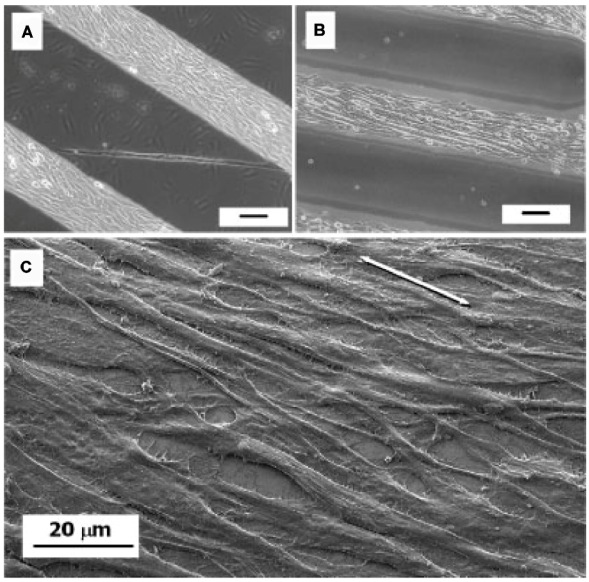
A
B
C
20 μm

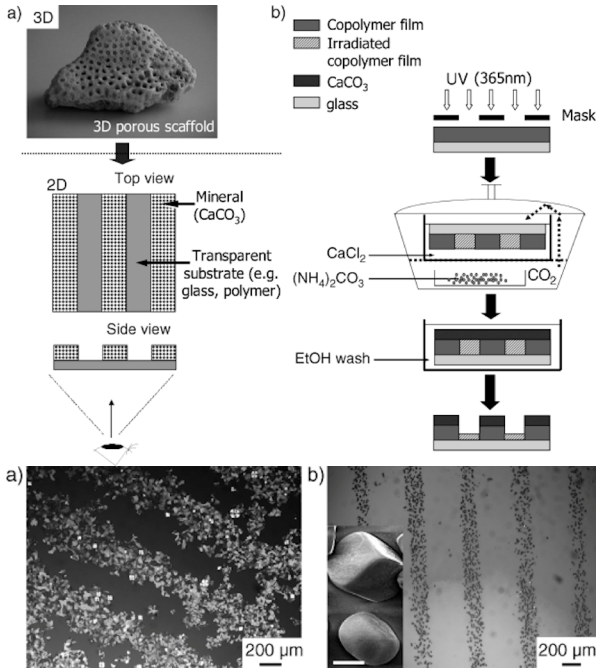
a)
3D
3D porous scaffold
2D
Top view
Mineral
($CaCO_3$)
Transparent
substrate (e.g.
glass, polymer)
Side view
b)
Copolymer film
Irradiated
copolymer film
$CaCO_3$
glass
UV (365nm)
Mask
$CaCl_2$
$(NH_4)_2CO_3$
CO_2
EtOH wash

a)
200 µm
b)
200 µm

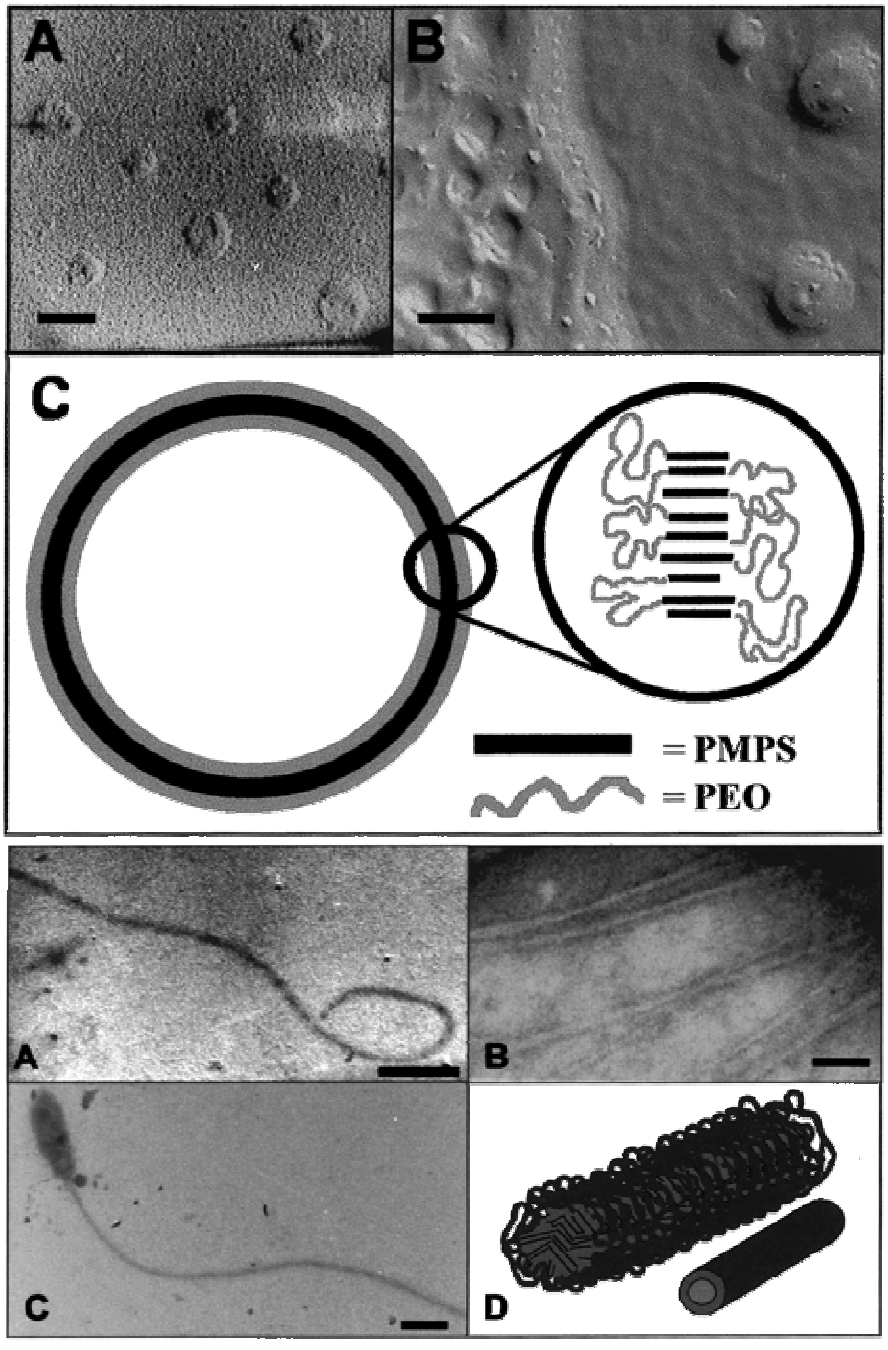
A
B
C
= PMPS
= PEO
A
B
C
D

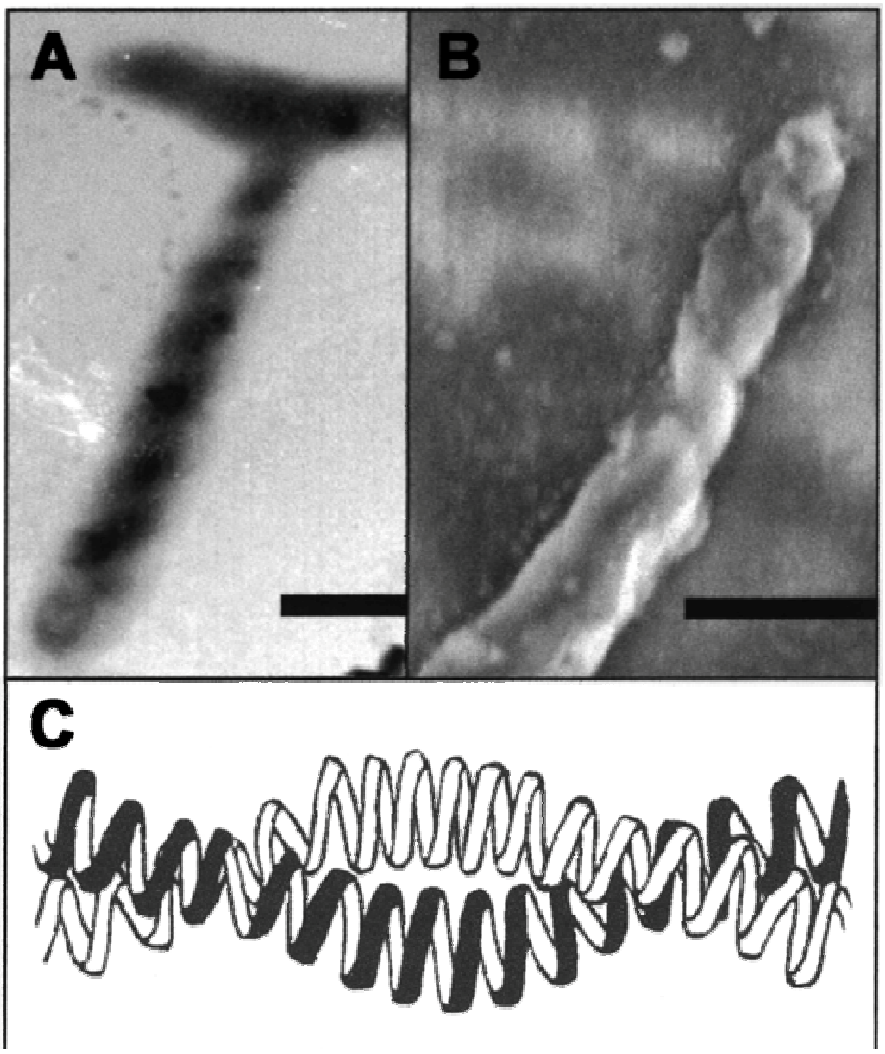
A
B
C

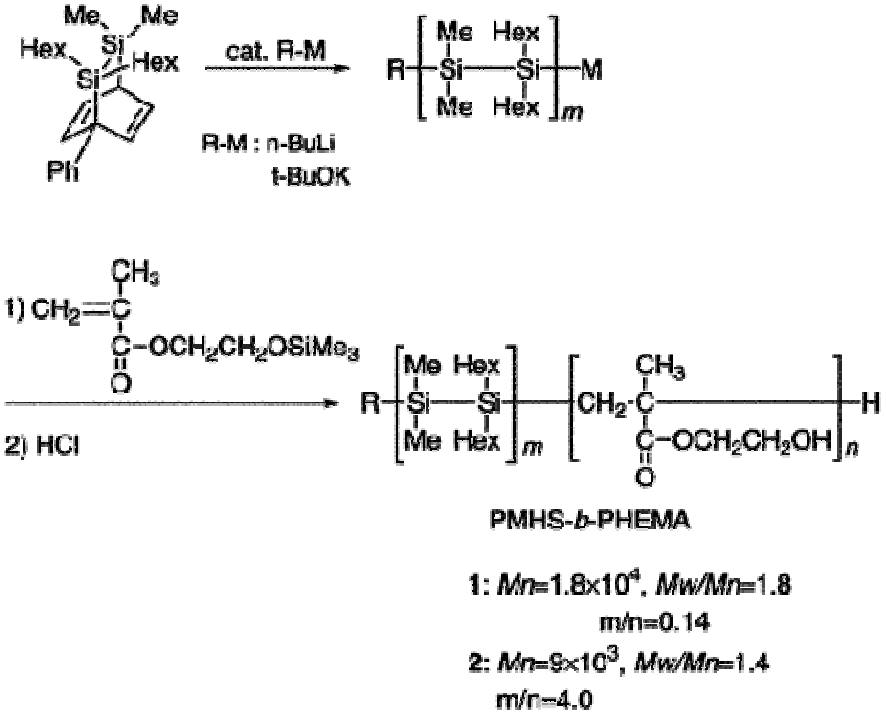

PMHS-*b*-PHEMA

1: Mn=1.8x10^4, Mw/Mn=1.8
m/n=0.14

2: Mn=9x10^3, Mw/Mn=1.4
m/n=4.0

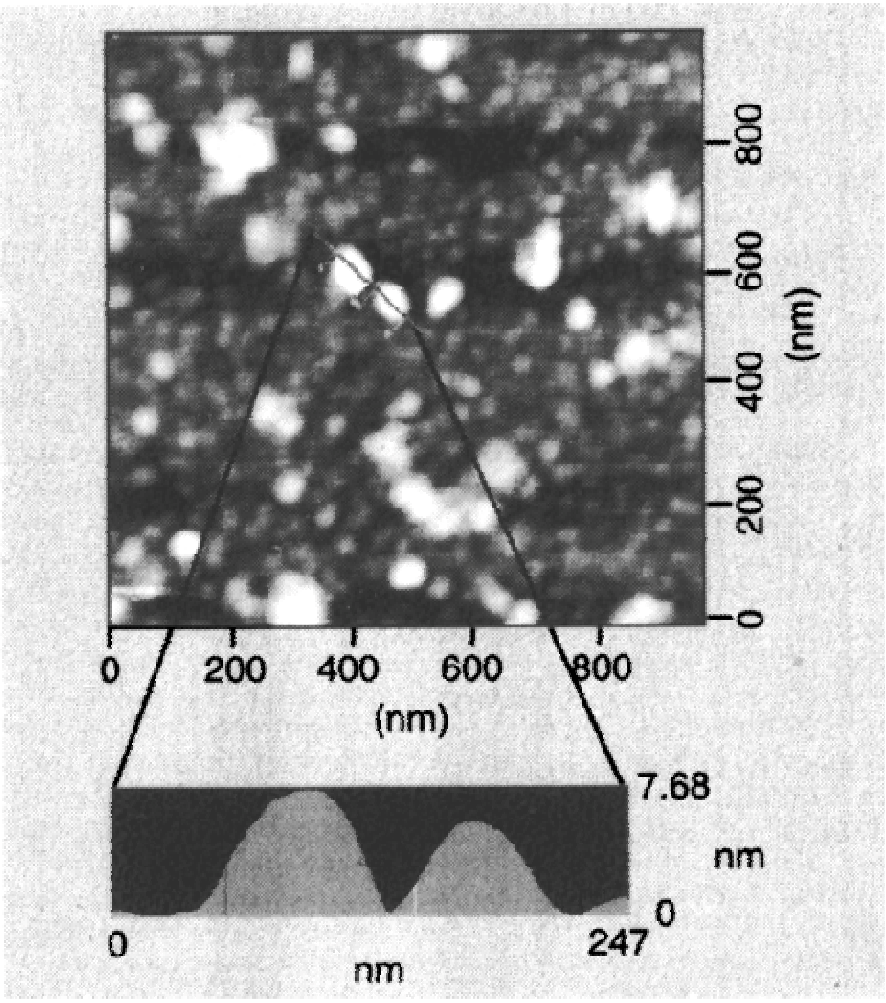
0
200
400
600
800
(nm)
0
200
400
600
800
(nm)
7.68
nm
0
0
247
nm

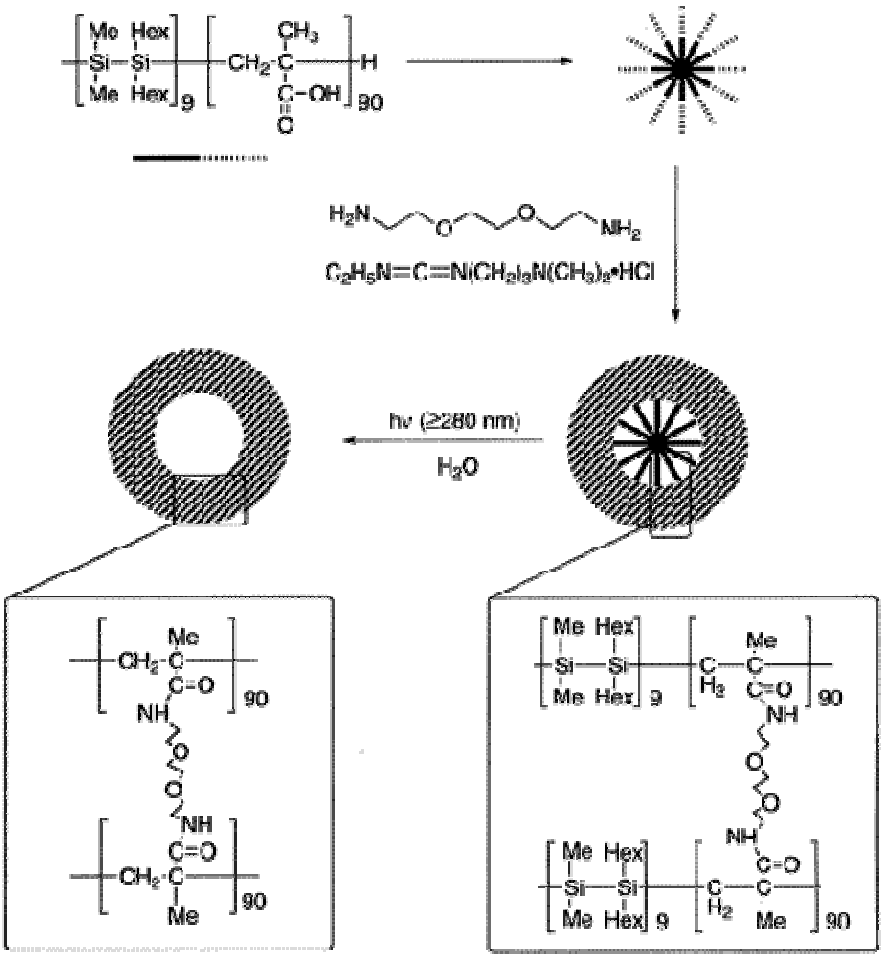
Me Hex
Si Si
Me Hex
9
CH2 C
CH3
C=O
OH
H
90
H2N
O
O
NH2
C2H5N=C=Ni(CH2)3N(CH3)2•HCl
hv (≥280 nm)
H2O
NH
C=O
CH2 C
Me
90

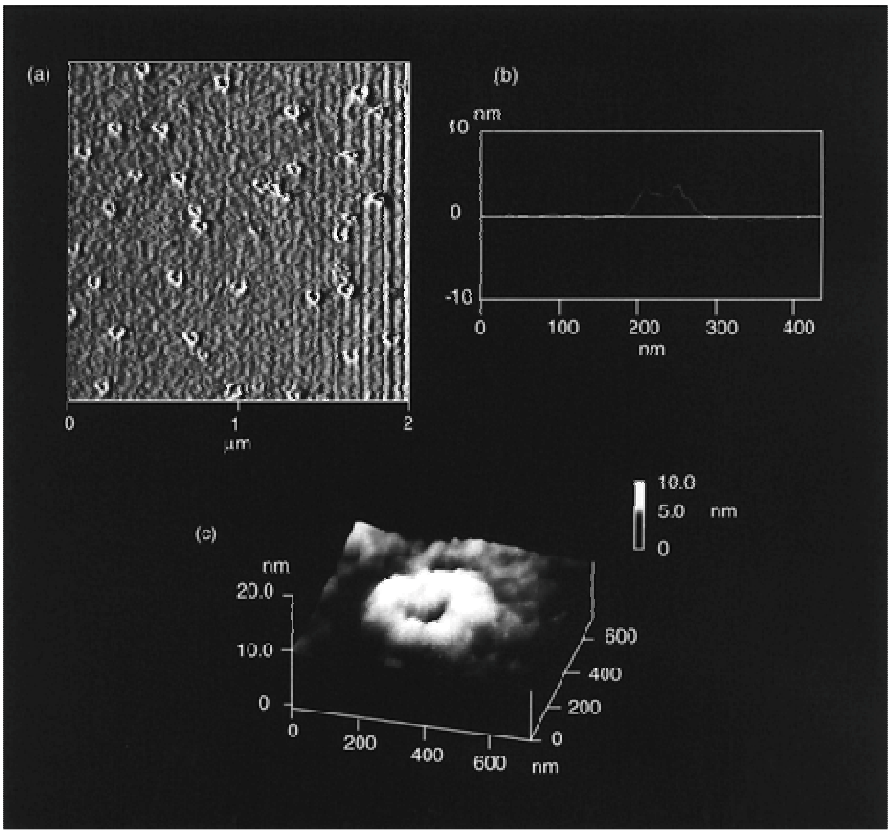
(a)
0
1
2
μm
(b)
nm
10
0
-10
0
100
200
300
400
nm
(c)
10.0
5.0
nm
0
nm
20.0
10.0
0
0
200
400
600
nm
600
400
200
0

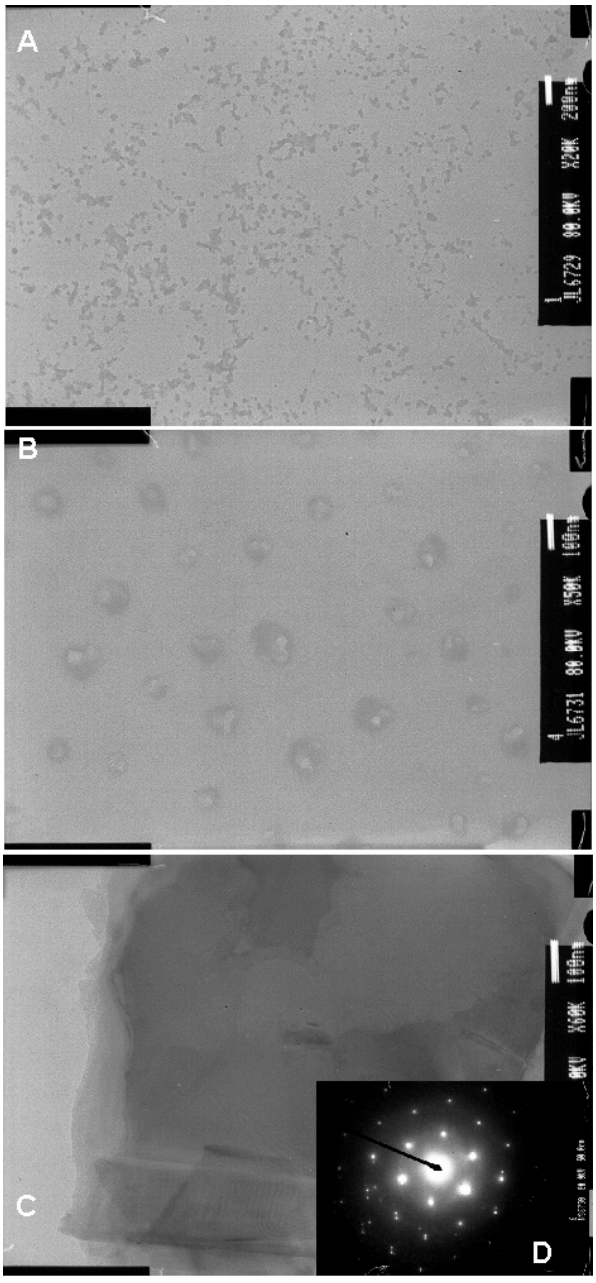
A
B
C
D

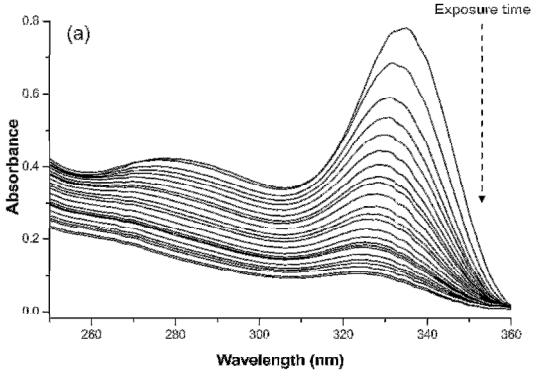
(a)
Exposure time
Absorbance
Wavelength (nm)

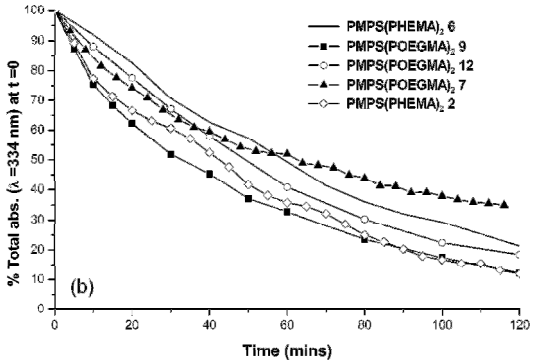
PMPS(PHEMA)2 6
PMPS(POEGMA)2 9
PMPS(POEGMA)2 12
PMPS(POEGMA)2 7
PMPS(PHEMA)2 2
% Total abs. (λ =334 nm) at t =0
Time (mins)
(b)

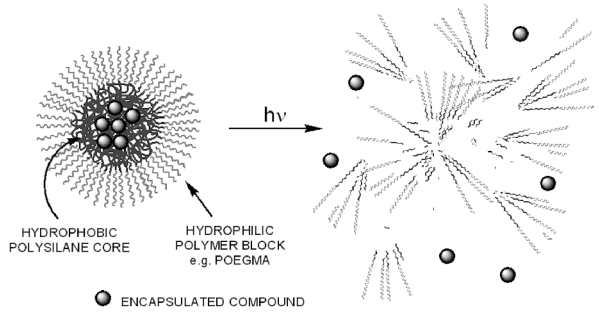
hν
HYDROPHOBIC
POLYSILANE CORE
HYDROPHILIC
POLYMER BLOCK
e.g. POEGMA
ENCAPSULATED COMPOUND